arXiv:1604.08890v1 [q-bio.BM] 28 Apr 2016

How did prebiotic polymers become informational foldamers?

Elizaveta A Guseva*
Laufer Center for Physical and Quantitative Biology, & Departments of Physics and Astronomy and Chemistry, Stony Brook University, Stony Brook, NY, (United States)

Ronald N Zuckermann
Lawrence Berkeley National Laboratory (LBNL), Berkeley, CA (United States)

Ken A Dill†
Laufer Center for Physical and Quantitative Biology, and Departments of Physics & Astronomy and Chemistry, Stony Brook University, Stony Brook, NY, (United States)

A mystery about the origins of life is which molecular structures – and what spontaneous processes – drove the autocatalytic transition from simple chemistry to biology? Using the HP lattice model of polymer sequence spaces leads to the prediction that random sequences of hydrophobic (H) and polar (P) monomers can collapse into relatively compact structures, exposing hydrophobic surfaces, acting as primitive versions of today's protein catalysts, elongating other such HP polymers, as ribosomes would now do. Such foldamer-catalysts form an autocatalytic set, growing short chains into longer chains that have particular sequences. The system has capacity for the multimodality: ability to settle at multiple distinct quasi-stable states characterized by different groups of dominating polymers. This is a testable mechanism that we believe is relevant to the early origins of life.

INTRODUCTION

Among the most interesting and mysterious processes in chemistry is how the spontaneous transition occured, more than 3 billion years ago, from a soup of prebiotic molecules to living systems. What was the mechanism of the Chemistry-to-Biology (CTB) transition? This is one of those scientific puzzles for which theory may be required to preceed experiments, even to suggest what mechanisms might be plausible. In this paper we develop a model to explore what prebiotic polymerization processes might have produced long chains of protein like or nucleic acid like molecules [1, 2]. What polymerization processes are autocatalytic? How could they have produced chains that are longer than are currently observed in model prebiotic experiments? And, how might random chain sequences have become informational and self-serving? Our questions here are about physical spontaneous mechanisms, not about the different chemistries of monomers or polymer types or polymerization conditions, *per se*.

THE CHEMISTRY-TO-BIOLOGY TRANSITION HAS BEEN POSTULATED TO ENTAIL AN AUTOCATALYTIC PROCESS

Early on, it was recognized that the transition to biological self-supporting behavior requires autocatalysis, *i.e.* some form of positive feedback or bootstrapping in which some molecules become amplified and self-sustaining relative to other molecules [3–8]. That work has led to the idea of an *autocatalytic set*, a collection of entities in which any one entity can be autocatalytic for another. We review here some of the key subsequent results, first from theory and modeling. A class of models called GARD (Graded Autocatalysis Replication Domain) [9–11] predicts that artificial autocatalytic chemico-kinetic networks can lead to self-replication, with a corresponding amplification of some chemicals over others. Such systems display some degree of inheritance and adaptability. GARD models are a subset of 'metabolism-first' mechanisms, which envision that small-molecule chemical processes precede information transfer and precede the first biopolymers. Focusing on polymers, Wu and Higgs [12] developed a model of RNA chain-length autocatalysis. They envision that some of the RNA chains can spontaneously serve as polymerase ribozymes, leading to autocatalytic elongation of other RNAs. A related model asserts that autocatalytic chain elongation arises from template-assisted ligation and random breakage [13]. These are models of the 'pre-informational' world before heteropolymers begin to encode biological sequence-structure relationships.

Another class of models describes a 'post-informational' heteropolymer world, in which there is already some tendency of chains to evolve. In one such model, it is assumed that polymers serve as their own templates because of the ability of certain heteropolymers to concentrate their own precursors [14–17]. It supposes an ability of molecules to recognize "self", although without specifying exactly how. In another such model [18], chains undergo sequence-independent

* eguseva@tutanota.com
† dill@laufercenter.org

template-directed replication. It indicates that functional sequences can arise from non-functional ones through effective exploration of sequence space. These post-informational models predict that template-directed replication will enhance sequence diversity [17]. These are abstract models that address matters of principle, rather than questions of what particular molecular structures might explain the autocatalytic step. Nor do they address the heteropolymeric or informational aspects of the chains.

There has also been much experimental work, leading, for example, to the creation of artificial autocatalytic sets in the laboratory [19–21]. Such systems are designed so that pairs of molecules can catalyze each other (i.e. autocatalysis), leading to exponential growth of the autocatalytic members. For example, mixtures of RNA fragments are shown to self-assemble spontaneously into self-replicating ribozymes that can form catalytic networks that can compete with others[22]. One limitation, however, is that these are fragments taken from existing ribozymes, so they don't explain the origins from more primitive and random beginnings.

Here, we describe a theoretical model that seeks to bridge from the pre- to post-informational world, across the Chemistry-to-Biology transition. We seek a physical basis for how short chains could have led to longer chains, for how random chains led to specific sequences, and for a structural basis and plausible kinetics for a prebiotic autocatalytic transition.

THE 'FLORY LENGTH PROBLEM': POLYMERIZATION PROCESSES PRODUCE MOSTLY SHORT CHAINS

Prebiotic polymerization experiments rarely produce long chains. It is commonly assumed that the chain lengths of proteins or nucleic acids that could have initiated the transition to biology must be at least 30-60 monomers long [23]. Both amino acids or nucleotides can polymerize under prebiotic conditions without enzymes, but they produce mostly short chains [24–28]. Leman et al. showed that carbonyl sulfide (COS), a simple volcanic gas, brings about the formation of oligo-peptides from amino acids under mild conditions in aqueous solution in minutes to hours. But the products are mainly dimers and trimers [27]. Longer chains can sometimes result through adsorption to clays [29, 30] or minerals [31, 32], from evaporation from tidal pools [33], from concentration in ice through eutectic melts [34], or from freezing [35] or temperature cycling. Even so, the chain-length extensions are modest.

For example, mixtures of Gly and Gly_2 grow to about 6-mers after 14 days [36, 37] on mineral catalysts such as calcium montmorillonite, hectorite, silica or alumina. Or, in the experiments of Kanavarioti, polymers of oligouridylates are found up to lengths of 11 bases long, with an average length of 4 [34] after samples of phosphoimidazolide-activated uridine we frozen in the presence of metal ions in dilute solutions. Similar results are found in other polymers: a prebiotically plausible mechanism produces oligomers having a combination of ester and amide bonds up to length 14 [38].

It is puzzling how prebiotic processes might have overcome what we call the "Flory Length Problem" – i.e. the tendency of any polymerization process to produce a distribution in which there are more short chains and fewer long chains. Standard polymerization mechanisms lead to the the Flory or Flory-Schulz distribution of populations $f(l)$, whereby short chains are exponentially more populated than longer chains [39],

$$f(l) = a^2 l (1-a)^{l-1}, \tag{1}$$

where l is the chain length and a is the probability that any monomer addition is a chain termination. The average chain length is given by $\langle l \rangle = a(2-a)$; see Figure 1(a).

Prebiotic monomer concentrations are thought to have been in the range of micromolar to millimolar [34, 40–43]. Given micromolar concentrations of monomers, and given $\langle l \rangle = 2$, the concentration of 40-mers would be $\approx 10^{-19}$ mol/L. Figure 1(b) shows that where the chain-length distributions are known for prebiotic syntheses, they are well fit by the Flory distribution (or exponential law $f(l) \propto \text{constant}^l$) [14, 17]).

THE FOLDAMER-AUTOCAT MECHANISM: SHORT HP CHAINS FOLD AND CATALYZE THE ELONGATION OF OTHER HP CHAINS

We propose that the key to the Chemistry-to-Biology transition may have been *foldable polymers* ('foldamers'). Today's biological foldamers are predominantly proteins (although RNA molecules and synthetic polymers can also fold [46–48]). Many foldamers adopt specific native conformations, mainly through a binary solvation code of particular sequence patternings of the H (hydrophobic) and P (polar) monomers [49]. We call these HP copolymers.

Since today's bio-catalysts are proteins, it is not hard to imagine that yesterday's primitive proteins could have been primitive catalysts. Precision and complexity are not required for peptides to perform biological functions. For example, proteins generated from random libraries can sustain the growth of living cells [50]. And, specific binding actions between random peptides and small molecules are not rare [51]. Below, we describe results of computer simulations that lead to the conclusion that short random HP chains carry within them the capacity to autocatalytically become longer and more protein-like.

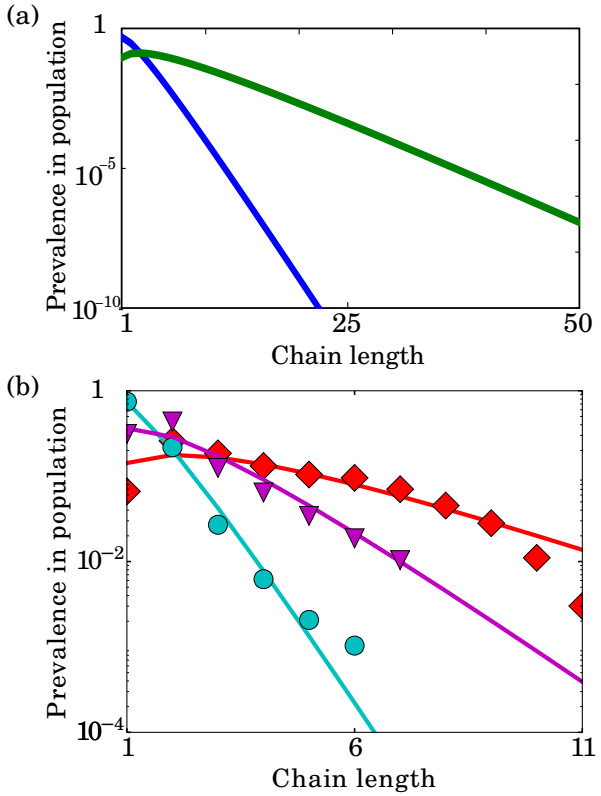

FIG. 1. **Polymerization processes lead to mostly short chains.** (a) Spontaneous polymerization processes typically lead to a Flory distribution of chain lengths. Green line gives $\langle l \rangle = 6$, blue corresponds to $\langle l \rangle = 2$ (b) Fitted distributions from experiments on prebiotic polymerization: red – Kanavarioti [34], cyan – Ding [44], magenta – Ferris [45]

Here are the premises of the model

1. Some random HP sequences can fold into compact structures.

2. Some of those foldamers will have exposed hydrophobic "landing pad" surfaces.

3. Foldamers with landing pads can catalyze the elongation of other HP chains.

4. These foldamer-catalysts form an autocatalytic set.

Here is evidence for these premises.

1. Non-designed random HP sequences are known to fold. HP polymers have been studied extensively as a model for the folding and evolution of proteins [49, 52–55]. Those studies show that folded structures can be encoded simply in the binary patterning of polar and hydrophobic residues, with finer tuning by specific interresidue contacts [56, 57]. This is confirmed by experiments [58–61].

2. Exposed hydrophobic clusters and patches are common on today's proteins. A study of 112 soluble monomeric proteins [62] found patches ranging from 200 to $1,200 \mathring{A}^2$, averaging around $400 \mathring{A}^2$; they are often binding sites for ligands or other proteins. Modern proteins have many sites of interaction with other proteins, typically nearly a dozen partners. Almost 3/4 of protein surfaces have geometrical properties that are amenable to interactions and those sites are enriched in hydrophobes [63].

3. Surface hydrophobic patches on proteins are often sites of catalysis [62, 64–66]. For example, hydrophobic clusters on the surface of lipases serve as initiation sites where the hydrophobic tail of a surfactant interacts with the patch first [65]. A hydrophobic cluster on Cytochrome-c Oxidase is known to increase k_{cat}[66].

4. Primitive proteins might have catalyzed peptide-chain elongation. Of course, today's cells synthesize proteins using ribosomes, wherein the catalysis is carried out by RNA molecules. Yet, there are reasons to believe that peptide chain elongation might alternatively be catalyzable by proteins. First, peptide chain elongation entails a condensation step and the removal of a water molecule [67, chapter 3, p. 82]. Dehydration reactions can occur in water if carried out in nonpolar environments [68, 69], such as protein surfaces. Second, a major route of protein synthesis in simple organisms such as bacteria and fungi utilizes nonribosomal peptide synthetases, and which don't involve mRNAs [70, 71].

MODELING THE DYNAMICS OF HP CHAIN GROWTH AND SELECTION

The dynamics of the model. We assume that chain polymerization takes place within a surrounding solution that contains a sufficient supply of activated H and P monomers. Since living systems – past or present – must be out-of-equilibrium, this assumption is not very restrictive. In our model, activated H and P monomers are supplied by an external source at rate a. A given chain elongates by adding a monomer at rate β. Just to keep the bookkeeping simple, we consider a steady state process in which molecules are removed from the system by degradation or dilution at the same rate they are synthesized. We assume chains can undergo spontaneous hydrolysis due to interaction with water; any bond can be broken at a rate h. Without loss of generality we define the unit rate by setting $\beta = 1$. All other rates are taken relative to this chain-growth rate.

Chain folding in the model. In addition, our model also allows for how the collapse properties of the different HP sequences affect the populations that polymerization produces. A standard way to study the properties of HP sequence spaces is using the 2D HP lattice model [49, 52].

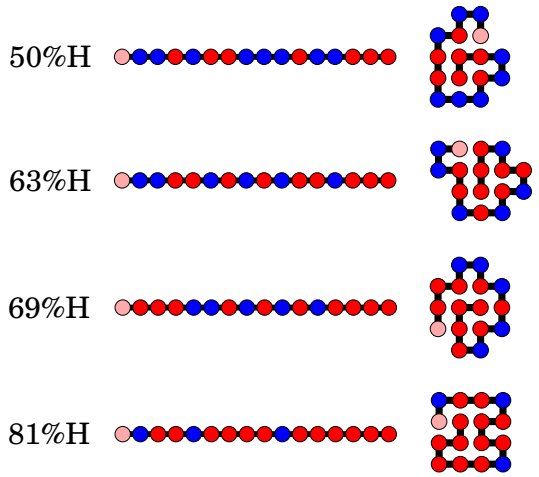

FIG. 2. **Examples of HP sequences that fold to unique native structures in the HP lattice model. Red (or pink if in the beginning of the sequence) corresponds H monomers and, blue to P.**

In this model, each monomer of the chain is represented as a bead. Each bead is either H or P. Chains have different conformations, represented on a 2-dimensional square lattice. The free energy of a given chain in a given conformation equals (the number of HH noncovalent contacts) $\times$ (the energy e_H of one HH interaction). Some HP sequences have a single lowest-free-energy structure, which we call *native*, having native energy E_{nat}:

$$E_{nat} = n_{h\phi} e_H. \qquad (2)$$

where $n_{h\phi}$ is the number of HH contacts in the native structure of that particular sequence.

A virtue of the HP lattice model is that for chains shorter than about 25 monomers long, every possible conformation of every possible sequence can be studied by exhaustive computer enumeration. Thus folding and collapse properties of whole sequence spaces can be studied without bias or parameters. Prior work shows that the HP lattice model reproduces many of the key observations of protein sequences, folding equilibria, and folding kinetics of proteins[72]. A main conclusion from previous studies is that a non-negligible fraction of all possible HP sequences can collapse into compact and structured and partially folded structures resembling native proteins [52]; see fig. 2. The reason that the 2-dimensionality adequately reflects properties of 3-dimensional proteins is because the determinative physics is in the surface-to-volume ratios (because the driving force is burial of H residues). And, it is helpful that the 10-30-mers that can be studied in 2D have the same surface-to-volume ratios as typical 3D proteins, which are 100-200-mers [73].

We assume that folded and unfolded states behave differently, as they do in modern proteins. We suppose that a folded chain is prevented from further growth, and also are protected from hydrolysis. This simply reflects that open chains are much more accessible to degradation from the solvent or adsorption onto surfaces than are folded chains. Even so, folding in our model is a reversible, as it is for natural proteins, so some small fraction of the time even folded chains are unfolded, and in that proportion, our model allows further growth or degradation. For this purpose, we estimate the folding and unfolding rate coefficients for any HP sequence as [74]:

$$\ln\left(\frac{k_f}{k_u}\right) = -\Delta G/kT = E_{nat}/kT - N \ln z, \qquad (3)$$

where z is the number of rotational degrees of freedom per peptide bond.

Catalysis in the model. Some HP sequences will fold to have exposed hydrophobic surfaces. These surfaces could act as primitive catalysts, as modern proteins do more optimally today. Fig. 3 illustrates a common mechanism of catalysts; namely translational localization of the reacting components. A protein A (the catalyst molecule) has a hydrophobic 'landing pad' to which a growing reactant chain B and a reactant monomer C will bind, localizing them long enough to form a bond that grows the chain. How much rate acceleration could such a localization give? Here is a rough estimate.

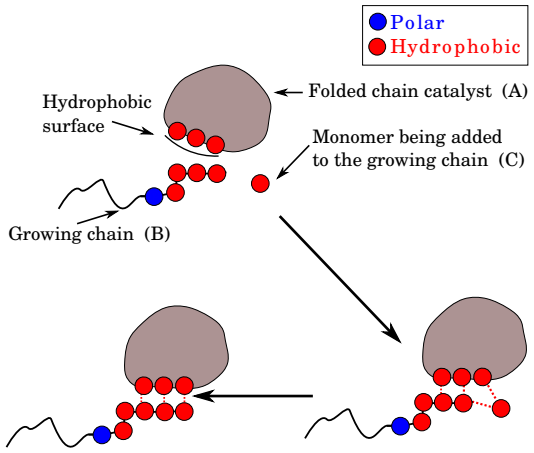

FIG. 3. **Some HP foldamers have hydrophobic patches, which serve as "landing pads" that can catalyze the elongation of other HP chains.** Chain A folds and exposes a hydrophobic sticky spot, or landing pad, where another HP molecule B, as well as an H monomer C, can bind. This localization reduces the barrier for adding monomer C to growing chain B.

For chain elongation, the catalytic rate will increase if the polymerization energy barrier is reduced by hydrophobic localization, by a factor $\beta_{\rm cat}/\beta_{\rm no\,cat} \propto \exp(E_H \cdot n_c/kT)$, where n_c is the number of H monomers in the landing pad (see figure 6). The free energy of a typical hydrophobic interaction is 1-2 kT. We take the minimum size of a landing pad to be 3. For a landing pad size of 3-4 hydrophobic monomers, this binding and localization would reduce the kinetic barrier by 3-8 kT, increasing the polymerization rate by 10x to 3000x. Of

course, this rate enhancement is much smaller than the 10^7-fold of modern ribosomes [75], but even small rate accelerations might have been relevant for prebiotic processes.

In order to simulate this dynamics, we run stochastic simulations. We used Expandable Partial Propensity Method (EPDM) [76]. Description and the corresponding C++ library, can be found at: https://github.com/abernatskiy/epdm.

RESULTS

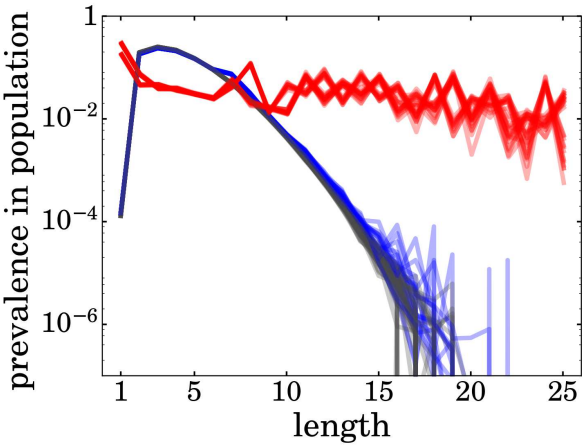

FIG. 4. **Chains become elongated by foldamer-catalyst HP sequences. Case 1 (gray): A soup of chains has a Flory-like length distribution in the absence of folding and catalysis. Case 2 (blue): A soup of chains still has a Flory-like length distribution in the absence of catalysis (but allowing now for folding). Case 3 (red): A soup of chains contains considerable populations of longer chains when the soup contains HP chains that can fold and catalyze. We run 30 simulations for every case. To produce each line we took a time average over 10^6 time points in the steady state interval, then counted molecules for each length and divided it it by the total molecular count.**

Folding alone does not solve the Flory Length Problem. But folding plus catalysis does.

We compare three cases: Case 1 is a reference test in which sequences grow and undergo hydrolysis but no other factors contribute, Case 2 allows for chain folding, but not for catalysis and Case 3 allows for both chain folding and catalysis. Case 1 simply recovers the Flory distribution, as expected, with exponentially decaying populations with chain length (see figure 4 gray lines). In the Case 2 when chains can fold, they can bury some monomers in their folded cores. So, chains that are compact or folded degrade more slowly than chains that don't fold. However, shows that this situation does not solve the Flory length problem either. Folding does increase the populations of some foldamer sequences relative to others, but the effects are too small affect the shape of the overall distribution (see figure 4 blue lines). Case 3 gives considerably larger populations of longer chains than cases 1 or 2 give (red lines on figure 4). When chains can both fold by themselves and also catalyze the elongation of others, such polymerization processes will "bend" the Flory distribution. This effect is robust over an order of magnitude of the hydrolysis and dilution parameters. The result is that some HP chains can fold, expose some hydrophobic surface, and reduce the kinetic barrier for elongating other chains. These enhanced populations of longer chains occur even though the degree of barrier reduction is relatively small.

Case 3 is qualitatively different than cases 1 and 2. Even though cases 1 and 2 have substantial variances, they have well-defined mean values that diminish exponentially with chain length. Case 3 has much bigger variances, and a polynomial distribution of chain lengths, so neither the mean nor median are good representations of the behavior of the chains; see figure 5(Case 3).

The foldamer-catalyst sequences form an autocatalytic set.

The present model makes specific predictions about what molecules constitutes the autocatalytic set – which HP sequences and native structures are in it, and which ones are not. Figure 6 shows a few of the HP sequences that fold to single native structures. Figure 6 (a) shows those foldamers that are catalysts while Figure 6 (b) shows those foldamers that are not catalysts.

In short, all HP sequences that are foldamer-catalysts are members of the autocatalytic set: any two HP foldamer-catalyst sequences are autocatalytic for each other. Figure 7 shows two examples of autocatalytic paired chain elongations. The top row of Figure 7 shows *crosscatalysis*: a polymer A elongates a polymer B while B is also able to elongate A. The bottom row of Figure 7 shows *autocatalysis*: one molecule C elongates a another C molecule in solution.

The size of the autocatalytic set grows with the size of the sequence space.

An important question is how the size of an autocatalytic set grows with the size of the sequence space. Imagine first the situation in which the chemistry-to-biology transition required one or two 'special' proteins as autocatalysts. This situation is untenable because sequence spaces grow exponentially with chain length. So, those few particular special sequences would wash out as biology moves into an increasingly larger sequence space 'sea'. In contrast, Figure 8 shows that the present mechanism resolves this problem. On the one hand, the frac-

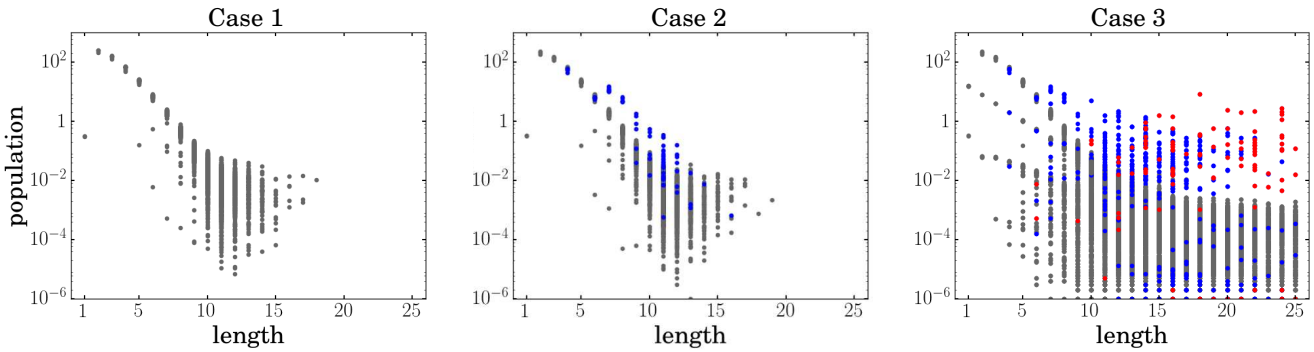

FIG. 5. **The distributions over individual sequences are highly heterogeneous. We show the populations (molecule counts of individual sequences) for the three cases: in case 1 we don't allow folding or catalysis, in case 2 we allow folding but not catalysis, and in case 3 both folding and catalysis are allowed. For all the cases gray dots represent populations of the sequences that cannot fold, blue – sequences that fold, but cannot catalyze and red – sequences which act as catalysts and for which at least one elongation reaction has been catalyzed. For cases 1 and 2, populations of the sequences of the given length are distributed exponentially. Thus we can take mean or median population for the given length as a faithful representation of the behavior of average sequence of that length. The case 3 is drastically different: the populations of the sequences of the given lengths are distributed polynomially. While most of the sequences have very low population for the longer chains, several sequences (mostly autocatalytic ones) have very high ones and constitute most of the biomass. For the case 3 neither mean or median are good representations of the behavior of the chains, as we can see from the figure, all the chains basically separate into two groups with different distributions, this information cannot be shown in the mean or median. Every point on the panels is a time average over 10^6 time points in the steady state interval. Lower limit of 10^{-6} is due to computational precision.**

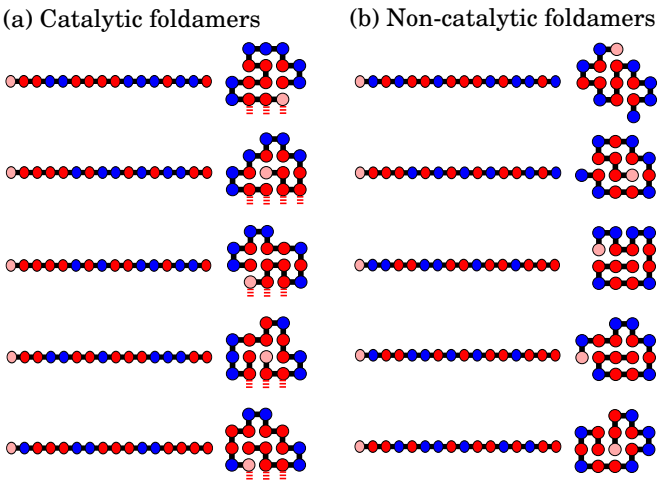

FIG. 6. **(a) HP lattice chains that fold and are autocatalytic.** They fold into unique structures and have landing pads that can catalyze the elongation of each other. **(b) HP chains that fold, but are not catalytic.** Most chains are not catalysts, but the size of the autocatalytic set is non-negligible; see Fig. 8.

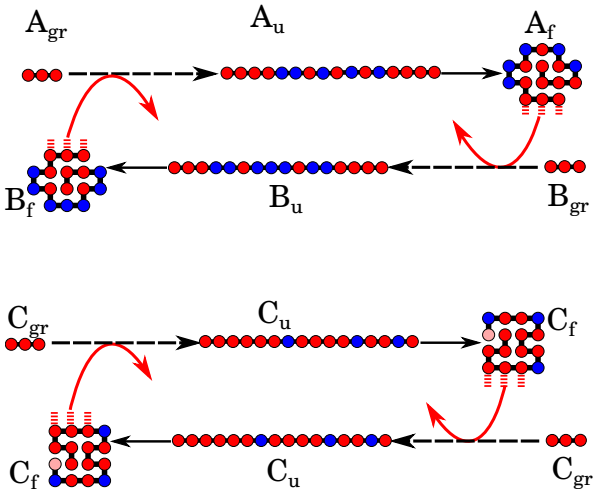

FIG. 7. **Top: Cross-catalysis of 2 different sequences. Bottom: Auto-catalysis of 2 copies of an identical sequence. Dashed arrows (- - -) represent multiple reactions of chain growth. Among them there are both $\cdots HH+H \rightarrow \cdots HHH$ catalyzed reactions and spontaneous chain elongations. Catalysis is represented by red solid arrows (—). Solid black lines (—) are folding reactions. Chains, which we call "autocatalytic" experience catalysis during one (or more often several) of the steps of elongation. Then, when they reach the length at which they can fold (A_u, B_u, C_u), they fold and serve as catalysts them selves (A_f, B_f, C_f). Mutual catalysis can happen between different sequences (here A and B) and between different instances of the same sequence (here C).**

tion of HP sequences that are foldamers is always fairly small (about 2.3% of the model sequence space), and the fraction of HP sequences that are also catalysts is even smaller (about 0.6% of sequence space). On the other hand, Figure 8 shows that the populations of both foldamers and foldamer-cats grow in proportion to the size of sequence space. The implication is that the space of autocats in the CTB might have been huge. Figure 9 makes a closely related point. It shows that for longer chains, the fraction of biomass that is produced by autocatalysts completely takes over and dominates the polymerization process, relative to just the basic polymeriza-

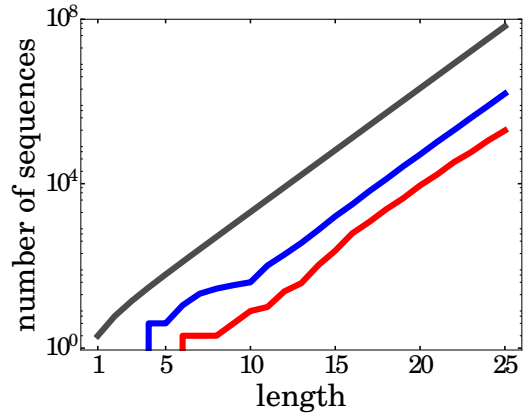

FIG. 8. **Different sequence spaces grow exponentially with chain length. (Gray) The number of all HP sequences. (Blue) The number of foldamers. (Red) The number of foldamer catalysts.**

tion dynamics itself, even though the catalytic enhancements are quite modest. This is due to two factors: (1) the number of autocatalysts grow longer sequences (see fig.8 and (2) folding alone is not sufficient to populate longer chains. We find that the average hydrophobicity of the dominant sequences in these runs is 68%.

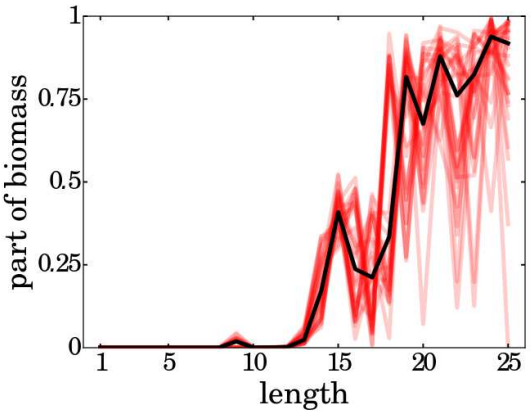

FIG. 9. **The longer chains the chains, the bigger the contribution of the autocatalysts.** Each red line shows how the contribution of autocatalytic chains to the biomass of the given length grows with chain length. Different red lines correspond to different simulation runs. The black line shows the median over 30 simulations.

Evolvability of HP ensembles

There are a few problems CTB models in general and autocatalytic models in particular encounter. One of them is lack of variability and evolvability. Due to the compositional bias or poor dynamical structure of the model such systems converge to one state (attractor or attractor basin) determined by internal dynamics of the system and do not response to directional selection (see discussions in [17, 77] for example). For a complex system that has many attractors a perturbation can move the system over a threshold to the basin of another attractor. This allows for exploration of the sequence space and thus possible evolvability of the system.

HP ensembles have, we believe, two possible attractors, which allow for the exploration of the sequence space. First, as one can see from the figure 10(a) trajectories split distinctively between two attraction distributions. There are no trajectories that lay in between the two attractors, which shows that there's no switching between the attractors and the separation is not result of stochasticity. In addition to that each of the distribution has a set of specific sequences which most often dominate the populations. Figure 10(b) shows a few of the structures dominating HP ensembles for the "green" distribution and for the "red" ones. The red and green species differ simply by different starting seeds for the simulations. Each of the two attractors has its own "signature ensemble" of HP sequences that is an emergent property of the dynamics. It is possible that adding more realism to our model (20 monomer types, rather than 2; allowing for longer chains; etc) could lead to larger numbers of attractors. Second, our simulations are limited to 25mers, but in fact the chains can grow longer. This fact allows for the further exploration of the sequence and functionality space beyond what can be seen in our simulations. If we are talking about protein-like molecules, some of the chains will act not only as autocats but also would be capable of binding other molecules, which could result in a chemical innovation.

At this point, we note what our model is, and what it is not. Our model is not intended as an accurate atomistic depiction of a real catalytic mechanism. It is a coarse-grained toy model, of which there will be variants. The mechanism we explore here is the translational localization of the two reactants, polymer B and monomer C, in the chain extension reaction. And, while this model is 2-dimensional, extensive previous studies have shown that it captures many important principles of folding and sequence-to-structure relationships. At the present time, this type of model is the only unbiased, complete and practical way to explore plausibilities of physical hypotheses such as the present one.

We note that the present model is not necessarily exclusive to proteins. Nucleic acid molecules are also able to fold in water, indicating differential solvation. While our present model focuses on hydrophobic interactions, it is simply intended as a concrete model of solvation, that could more broadly include hydrogen bonding or other interactions. So, while our analysis here is only applicable to foldamers, that does not mean it is limited to proteins. The unique power that foldable molecules have for catalyzing reactions – in contrast to other nonfoldable polymeric structures – is that foldamers lead to precisely fixing atomic interrelationships in relative stable ways

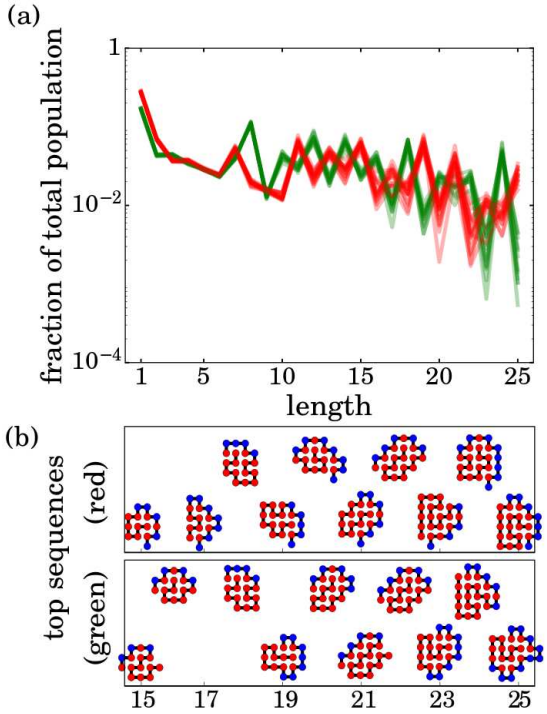

FIG. 10. (a) *HP* catalytic system has at least two attractors. The lines are length distributions from case 3. Again, each line represents distribution of length in the steady state for one simulation run. It is clear, that there are two kinds of distribution which get realized during the simulations. The system bifurcates either to a state represented by a green line or to one represented by red one. These are the same lines as on figure 5(a), but separated in two sets by the clustering algorithm k-means. (b) Structure of the sequences which most often are main contributors into the total population of the polymers of their length. Top panel corresponds to the macrostate shown in red on the panel (a), lower one, to the one shown in green.

over the folding time of the molecule. It resembles a microscale solid, with the capability that substrates and transition states can recognize, bind, and react to those stable surfaces. For example, serine proteases utilize a catalytic triad of 3 amino acids. So, foldability in some type of prebiotic polymer, could conceivably have had a special role in allowing for primitive catalysis. Here, we use a toy model to capture that simple idea, namely that a folded polymer can position a small number of residues in a way that can catalyze a reaction.

CONCLUSIONS

It has been recognized that life's origins require some form of autocatalysis [5, 6, 8]. But, what molecular structural mechanism might explain it? Here, we find that autocatalysis is inherent in the following process (see Figure 7): HP polymers are synthesized randomly; a small fraction of those HP polymers fold into relatively stable compact states; a fraction of those folded structures provide relatively stable 'landing pad' hydrophobic surfaces; those surfaces can help to catalyze the elongation of other HP molecules having foldable sequences.

The HP model allows for unbiased counting of sequences that do fold, don't fold, or fold and have a potentially catalytic hydrophobic landing pad. A non-negligible fraction of all possible HP sequences fold to unique structures (2.3% for lengths up to 25-mers). The fraction of all possible HP sequences that have catalytic surfaces (as defined above) is 12.7% of foldable sequences, or 0.3% of the whole sequence space. These ratios remain relatively constant with chain length, at least up to 25-mers; see figure 8. This and successful designs of foldable, biologically active proteins based on the HP folding rule [78] suggests that folding in HP polymers is not rare. The present model provides an experimentally testable prediction for what early polymer sequences could be autocatalytic, and provides a structural and kinetic mechanism for their action.

ACKNOWLEDGMENTS

Authors appreciate support from the Laufer Center as well as from NSF grant MCB1344230. Special thanks to Anton Bernatskiy for fruitful discussions.

SI: SIMULATIONS

To perform our stochastic simulations, we first needed to develop appropriate simulation code because of the large numbers of different molecular species that must be treated here. A description of the method, called the Expandable Partial Propensity Method (EPDM), and the corresponding C++ library, can be found at: https://github.com/abernatskiy/epdm [76]. The challenge is to keep track of all the molecular species and to search the full conformational spaces of each chain. This is NP-hard. We use the HP Sandbox algorithm[52, 79] [80], which is limited to maximum chain lengths of 25 monomers. To handle computational limitations, we restricted the total number of species to the level of a few thousands. We impose this limit by introducing a dilution parameter d: molecules are randomly removed from the system with probability $\propto d$. Physically, it represents molecules that diffuse out of the reaction volume. The total numbers of molecules within the reaction volume vary in the range of $10^2 - 10^4$. We start our simulations with a small pool of monomers, usually fewer than 100 molecules. Here are the dynamical steps:

- Polymerization happens when monomers react with other monomers or polymers at a rate $\beta = 1$:

$$1\text{-mer} + n\text{-mer} \xrightarrow{\beta} (n+1)\text{mer} \tag{4}$$

- New monomers are imported into the system at high rate $a \gg 1$.

$$\emptyset \xrightarrow{a} H \text{ or } P \tag{5}$$

- We assume a chain can break at any internal site by hydrolysis. This happens with rate h per chain bond.

$$n\text{-mer} \xrightarrow{h} l\text{-mer} + (n-l)\text{-mer} \tag{6}$$

  Typical values for the half-time for the hydrolysis of a bond under neutral conditions and room temperature are on the order of hundreds of years[81]. Here, we explored a range of hydrolysis rates that are about $0.01 - 1$ of the polymerization rate. Hence, our model polymerization rates are on the order of days to years.

- We assume the system becomes diluted, at rate d. This has the practical purpose of limiting the total population of polymer in the system. We explored values of d from $\propto 0.01 - 1\beta$. Given the values of a we used, it results in $\propto 10^2 - 10^4$ chains in the simulation volume.

$$\text{anything} \xrightarrow{d} \emptyset \tag{7}$$

- Folding and unfolding reactions happen much faster than the polymerization processes, with corresponding rate coefficients of $k_f \gg k_u \gg \beta$:

$$\begin{aligned} \text{folded chain} &\xrightarrow{k_u} \text{unfolded chain} \\ \text{unfolded chain} &\xrightarrow{k_f} \text{folded chain} \end{aligned} \tag{8}$$

  We used the most realistic values we could obtain for these rates and for the folding free energies for proteins. We took E_{nat} from the HP model, known folding free energies from experimental data [82, 83], and we used the relationship [74]:

$$\ln\left(\frac{k_f}{k_u}\right) = -\Delta G/kT = E_{nat}/kT - N\ln z, \tag{9}$$

  where z is the number of rotational degrees of freedom per peptide bond. To account for the difference between the 2D model and real 3D proteins, we calibrated the parameters taken from the literature to yield unfolding/folding rates that are meaningful in the context of the other rates in our model: folding is much faster than growth and for any of the sequence in our pool $k_f/k_u \in (10^2, 10^4)$ [82, 83] for 3D proteins. Because the literature models are only mean-field, averaged over sequences, and in order to retain sequence dependence here, we set the unfolding rate of all sequences to the average for their lengths, and assigned all the sequence dependence to k_f. So, we used: significantly.

$$\begin{aligned} k_u &= \exp[12 - 0.1\sqrt{N} - E_H(0.5N + 1.34)], \\ k_f &= k_u \exp(\Delta G) \end{aligned} \tag{10}$$

  The model is not sensitive to varying these parameters over a wide range. We use $E_h \approx 1 - 2\text{kT}$, so $k_{unf} \approx 10^2$, which leads to a range of unfolding rates from a reaction per hours and days and range of folding rates from a reaction per hours to fractions of a second.

- The catalytic step is:

$$\text{Catalyst} + H + \underbrace{\cdots HH}_{l-1} \xrightarrow{\beta_{cat}} \text{Catalyst} + \underbrace{\cdots HHH}. \tag{11}$$

  The rate enhancement is $\beta_{cat} = \beta \cdot \exp(E_h \cdot n_c/kT)$, where hydrophobic sticking energy is e_H, the number of contacting hydrophobes is n_c, which varies in the range $3 - 6$. With the hydrophobic energies of $e_H = 1 - 2\text{kT}$, this gives catalysis rates around hours to days per reaction. Because the EPDM supports only binary reactions, we divided the reaction above into to steps: interaction of catalyst with a monomer with rate β and the reaction of this complex with a polymer has the rate β_{cat}.

For each trajectory, we collected statistics only after the system reached an unchanging steady state. In order

to explore the stochasticity, we repeated every simulation for 30 times for every experiment. We ran all the simulations for $140s$ of internal simulation time, during which $10^6 - 10^9$ individual reactions had occurred. We took measurements every $10^{-6}s$. For all the trajectories steady state behavior was reached no longer than $40s$ after the start of a simulation. Thus we considered only the last $100s$ (one million recordings) for each simulation. All the data points we used in the figures are averages over these recordings.

For all the experiments below, we used the following parameters:

1. $\beta = 1$
2. $E_h = 2kT$
3. $z = 1.2$
4. $a = 1000$

   Values of $a \ll 1000$ or $a \gg 1000$ are problematic, having numbers of sequences or populations either too high to calculate or too low to draw conclusions.

5. $h = d = 0.1$.

   When $3d \lessapprox h \leq \beta$, hydrolysis is dominates and without catalysis, there's an explosion of short sequences.

   When $3h \lessapprox d \leq \beta$, hydrolysis is unphysically small, so nothing limits the growth of longer sequences, even in the absence of catalysis.

   When $0.05 \lessapprox d \approx h \lessapprox 0.5$ the forces of dilution and hydrolysis are relatively balanced and populations are neither too small or too large.

In-silico experiments

The simulations were performed on the Laufer Center's computing cluster of CPUs. Source files of the models, parameters, initial conditions and random seeds can be obtained at `https://github.com/gelisa/hp_world_data`. We performed the following computational experiments:

Experiment 1: Does our bare polymerization reproduce the Flory distribution? We started simulations with a small pool of chains up to 3-mers. To calculate the length distributions, we calculated for each trajectory the average population of every sequence over time over all recordings after 40s, resulting in a million time steps. Then we summed all the populations of a given length, obtained total populations for all n-mers, $n \in [1, 25]$, and then computed every population as:

$$p_n = \frac{\sum \text{all n-mers}}{\sum \text{total population}} \tag{12}$$

giving probability of finding an n-mer of a randomly chosen molecule in the system.

The source file of the model and parameters of the simulation are located at `https://github.com/gelisa/hp_world_data/tree/master/001`

Experiment 2. What is the effect on the distribution of just HP folding? We started with the same initial population as in Experiment 1. But now we introduce the hydrophobic energy $e_h = 2kT$. To calculate the resultin length distribution, we computed the average population of every sequence for each trajectory over time over all the recordings after 40s, resulting in a million time steps. The source file of the model and parameters of the simulation are located at `https://github.com/gelisa/hp_world_data/tree/master/002`

Experiment 3. What is the effect on the distribution of both folding and catalysis? In addition to folding in this *in-silico* experiment, we also accounted for the pairwise contact interactions between two proteins, with the parameters as indicated above. We explored ranges of parameters. We observed significant stability of the length distribution towards change of h and d: $0.05 \lessapprox d \approx h \lessapprox 0.5$. The distributions we observe are quite sensitive to the choice of hydrophobic energy, as expected for chemical reactions, since this enters into the exponent of the rate expression. In the generally physical range of $e_h = 1 - 3kT$, we observe a bending of the Flory distribution, as noted in the text. The source file of the model and parameters of the simulation are located at `https://github.com/gelisa/hp_world_data/tree/master/003`

[1] Joyce, G. *Cold Spring Harbor Symposia on Quantitative Biology* **1987**, *52*, 41–51.
[2] Abel, D. L.; Trevors, J. T. *Theoretical Biology and Medical Modelling* **2005**, *2*, 29.
[3] Eigen, M. *Die Naturwissenschaften* **1971**, *58*, 465–523.
[4] Eigen, M.; Schuster, P. *Naturwissenschaften* **1977**, *64*, 541–565.
[5] Eigen, M.; Schuster, P. *Naturwissenschaften* **1978**, *65*, 7–41.
[6] Dyson, F. *Origins of Life*; Cambridge: University Press, 1985.
[7] Prigogine, I.; Nicolis, G. *Exploring Complexity*; 1989.
[8] Kauffman, S. A. *Journal of Theoretical Biology* **1986**, *119*, 1–24.
[9] Segré, D.; Lancet, D.; Kedem, O.; Pilpel, Y. *Origins of Life and Evolution of the Biosphere* **1998**, *28*, 501–514.
[10] Segré, D.; Ben-Eli, D.; Lancet, D. *Proceedings of the National Academy of Sciences of the United States of Amer-*

ica **2000**, *97*, 4112–7.
[11] Markovitch, O.; Lancet, D. *Artificial life* **2012**, *18*, 243–66.
[12] Wu, M.; Higgs, P. G. *Journal of molecular evolution* **2009**, *69*, 541–54.
[13] Tkachenko, A. V.; Maslov, S. **2014**, 21.
[14] Nowak, M. A.; Ohtsuki, H. *Proceedings of the National Academy of Sciences* **2008**, *105*, 14924–14927.
[15] Ohtsuki, H.; Nowak, M. A. *Proceedings. Biological sciences / The Royal Society* **2009**, *276*, 3783–90.
[16] Chen, I. A.; Nowak, M. A. *Accounts of chemical research* **2012**, *45*.
[17] Derr, J.; Manapat, M. L.; Rajamani, S.; Leu, K.; Xulvi-Brunet, R.; Joseph, I.; Nowak, M. A.; Chen, I. A. *Nucleic acids research* **2012**, *40*, 4711–22.
[18] Walker, S. I.; Grover, M. A.; Hud, N. V. *PloS one* **2012**, *7*, e34166.
[19] von Kiedrowski, G. *Angewandte Chemie International Edition in English* **1986**, *25*, 932–935.
[20] Lincoln, T. A.; Joyce, G. F. *Science* **2009**, *323*, 1229–1232.
[21] Vaidya, N.; Manapat, M. L.; Chen, I. A.; Xulvi-Brunet, R.; Hayden, E. J.; Lehman, N. *Nature* **2012**, *491*, 72–7.
[22] Robertson, M. P.; Joyce, G. F. *Chemistry & biology* **2014**, *21*, 238–45.
[23] Szostak, J. W.; Ellington, A. D. *The RNA World*; Cold Spring Harbor Laboratory Press, 1993; pp 511–533.
[24] Shock, E. L. Stability of peptides in high-temperature aqueous solutions. 1992.
[25] Martin, R. B. *Biopolymers* **1998**, *45*, 351–353.
[26] Paecht-Horowitz, M.; Berger, J.; Katchalsky, A. *Nature* **1970**, *228*, 636–639.
[27] Leman, L.; Orgel, L. E.; Ghadiri, M. R. *Science (New York, N.Y.)* **2004**, *306*, 283–6.
[28] Orgel, L. E. *Critical reviews in biochemistry and molecular biology* **2004**, *39*, 99–123.
[29] Rao, M.; Odom, D. G.; Oró, J. *Journal of Molecular Evolution* **1980**, *15*, 317–331.
[30] Lambert, J.-F. *Origins of life and evolution of the biosphere : the journal of the International Society for the Study of the Origin of Life* **2008**, *38*, 211–42.
[31] Bernal, J. D. *Proceedings of the Physical Society. Section B* **1949**, *62*, 597–618.
[32] Ferris, J. P.; Hill, A. R.; Liu, R.; Orgel, L. E. *Nature* **1996**, *381*, 59–61.
[33] Nelson, K. E.; Robertson, M. P.; Levy, M.; Miller, S. L. *Origins of Life and Evolution of the Biosphere* **2001**, *31*, 221–229.
[34] Kanavarioti, A.; Monnard, P.-A.; Deamer, D. W. *Astrobiology* **2001**, *1*, 271–281.
[35] Bada, J. L. *Earth and Planetary Science Letters* **2004**, *226*, 1–15.
[36] Rode, B. M.; Son, H. L.; Suwannachot, Y.; Bujdak, J. **1997**, 273–286.
[37] Rode, B. M. *Peptides* **1999**, *20*, 773–786.
[38] Forsythe, J. G.; Yu, S.-S. S.; Mamajanov, I.; Grover, M. A.; Krishnamurthy, R.; Fernandez, F. M.; Hud, N. V.; Fern??ndez, F. M.; Hud, N. V. *Angew Chem Int Ed Engl* **2015**, *10*, n/a???n/a.
[39] Flory, P. J. *Principles of polymer chemistry*; Ithaca, NY : Cornell Univ., 1953; p 688.
[40] Stribling, R.; Miller, S. L. *Origins of Life and Evolution of the Biosphere* **1987**, *17*, 261–273.
[41] Huber, C.; Wächtershäuser, G. *Science (New York, N.Y.)* **1998**, *281*, 670–672.
[42] Aubrey, A. D.; Cleaves, H. J.; Bada, J. L. *Origins of Life and Evolution of Biospheres* **2009**, *39*, 91–108.
[43] Lazcano, A.; Miller, S. L. *Cell* **1996**, *85*, 793–798.
[44] Ding, P. Z.; Kawamura, K.; Ferris, J. P. *Origins of Life and Evolution of the Biosphere* **1996**, *26*, 151–171.
[45] Ferris, J. P. *Biological Bulletin* **1999**, *196*, 311.
[46] Gellman, S. H. *Accounts of Chemical Research* **1998**, *31*, 173–180.
[47] Lee, B.-C.; Zuckermann, R. N.; Dill, K. A. *J. Am. Chem. Soc.* **2005**, *127*, 10999–11009.
[48] Capriotti, E.; Marti-Renom, M. A. *Bioinformatics* **2008**, *24*, i112–i118.
[49] Chan, H. S.; Dill, K. A. *The Journal of Chemical Physics* **1991**, *95*, 3775.
[50] Fisher, M. a.; McKinley, K. L.; Bradley, L. H.; Viola, S. R.; Hecht, M. H. *PLoS ONE* **2011**, *6*, e15364.
[51] Cherny, I.; Korolev, M.; Koehler, A. N.; Hecht, M. H. *ACS synthetic biology* **2012**, *1*, 130–8.
[52] Lau, K. F.; Dill, K. A. *Macromolecules* **1989**, *22*, 3986–3997.
[53] Miller, D. W.; Dill, K. A. *Protein science : a publication of the Protein Society* **1995**, *4*, 1860–73.
[54] Yue, K.; Dill, K. A. *Proc Natl Acad Sci U S A* **1995**, *92*, 146–150.
[55] Agarwala, R.; Batzoglou, S.; Dancik, V.; Decatur, S. E.; Hannenhalli, S.; Farach, M.; MUTHUKRISHNAN, S.; SKIENA, S. *Journal of Computational Biology* **1997**, *4*, 275–296.
[56] Yue, K.; Dill, K. a. *Proceedings of the National Academy of Sciences of the United States of America* **1992**, *89*, 4163–4167.
[57] Xiong, H.; Buckwalter, B. L.; Shieh, H. M.; Hecht, M. H. *Proceedings of the National Academy of Sciences of the United States of America* **1995**, *92*, 6349–53.
[58] Lim, W. A.; Sauer, R. T. *Journal of Molecular Biology* **1991**, *219*, 359–376.
[59] Kamtekar, S.; Schiffer, J. M.; Xiong, H.; Babik, J. M.; Hecht, M. H. *Science (New York, N.Y.)* **1993**, *262*, 1680–1685.
[60] Wei, Y. *Protein Science* **2003**, *12*, 92–102.
[61] Brisendine, J. M.; Koder, R. L. *Biochimica et Biophysica Acta (BBA) - Bioenergetics* **2015**,
[62] Lijnzaad, P.; Berendsen, H. J. C.; Argos, P. *Proteins: Structure, Function and Genetics* **1996**, *25*, 389–397.
[63] Tonddast-Navaei, S.; Skolnick, J. *Journal of Chemical Physics* **2015**, *143*.
[64] Mitchell Guss, J.; Freeman, H. C. *Journal of Molecular Biology* **1983**, *169*, 521–563.
[65] van Ee, J. H.; Onno, M. In *Enzymes in Detergency*; van Ee, J. H., Ed.; CRC Press, 1997; p 408.
[66] Witt, H. *Journal of Biological Chemistry* **1998**, *273*, 5132–5136.
[67] Nelson, D. L.; Cox, M. M. *Lehninger Principles of Biochemistry*, 5th ed.; W. H. Freeman, 2008.
[68] Manabe, K.; Sun, X. M.; Kobayashi, S. *Journal of the American Chemical Society* **2001**, *123*, 10101–10102.
[69] Manabe, K.; Iimura, S.; Sun, X. M.; Kobayashi, S. *Journal of the American Chemical Society* **2002**, *124*, 11971–11978.
[70] Stachelhaus, T.; Mootz, H. D.; Bergendahl, V.; Marahiel, M. A. *Journal of Biological Chemistry* **1998**, *273*, 22773–22781.

[71] Marahiel, M. A. *Journal of peptide science : an official publication of the European Peptide Society* **2009**, *15*, 799–807.

[72] Dill, K. A. *Protein Science* **1999**, *8*, 1166–1180.

[73] Giugliarelli, G.; Micheletti, C.; Banavar, J. R.; Maritan, A. *Journal of Chemical Physics* **2000**, *113*, 5072–5077.

[74] Ghosh, K.; Dill, K. A. *Proceedings of the National Academy of Sciences of the United States of America* **2009**, *106*, 10649–54.

[75] Sievers, A.; Beringer, M.; Rodnina, M. V.; Wolfenden, R. *Proceedings of the National Academy of Sciences* **2004**, *101*, 7897–7901.

[76] Berntaskiy, A.; Guseva, E. **2016**,

[77] Vasas, V.; Fernando, C.; Szilágyi, A.; Zachár, I.; Santos, M.; Szathmáry, E. *Journal of Theoretical Biology* **2015**, *381*, 29–38.

[78] Murphy, G. S.; Greisman, J. B.; Hecht, M. H. *Journal of molecular biology* **2015**, *428*, 399–411.

[79] Dill, K. A.; Bromberg, S.; Yue, K.; Chan, H. S.; Ftebig, K. M.; Yee, D. P.; Thomas, P. D.; Fiebig, K. M.; Yee, D. P.; Thomas, P. D. *Protein Science* **2008**, *4*, 561–602.

[80] A Python implementation and description can be found at: http://hp-lattice.readthedocs.org/en/latest/.

[81] The hydrolysis rate constants of oligopeptides in neutral conditions are of the order of $10^{-11} - 10^{-10}$: $1.310^{-10} M^{-1} s^{-1}$ for benzoylglycylphenylalanine ($t_{1/2} = 128y$)[84], $6.310^{-11} M^{-1} s^{-1} (t_{1/2} = 350y)$ for glycylglycine and $9.310^{-11} M^{-1} s^{-1}$ for glycylvaline [85].

[82] Ghosh, K.; Dill, K. A. *Biophysical Journal* **2010**, *99*, 3996–4002.

[83] Dill, K. A.; Ghosh, K.; Schmit, J. D. *Proceedings of the National Academy of Sciences of the United States of America* **2011**, *108*, 17876–82.

[84] Bryant, R. A. R.; Hansen, D. E. *Journal of the American Chemical Society* **1996**, *118*, 5498–5499.

[85] Smith, R. M.; Hansen, D. E. *Journal of the American Chemical Society* **1998**, *120*, 8910–8913.